An Acad Bras Cienc (2021) 93(1): e20200178 DOI 10.1590/0001-3765202120200178
Anais da Academia Brasileira de Ciências | *Annals of the Brazilian Academy of Sciences*
Printed ISSN 0001-3765 I Online ISSN 1678-2690
www.scielo.br/aabc | www.fb.com/aabcjournal

GEOSCIENCES

Interpretation of geophysical data for iron ore detailed survey in Laje, Bahia, Brazil

EDSON E.S. SAMPAIO, JOELSON C. BATISTA & EMERSON S.M. SANTOS

Abstract: The transition zone between the Archean blocks, Jequié and Itabuna-Salvador-Curaçá, in the county of Laje, Bahia, Brazil, is potentially important for iron ore deposits of economic interest. This research investigates one of the eighteen anomalies defined by a previous integrated interpretation of geological and airborne gamma ray spectrometry and magnetic data in this transition zone. Its choice resulted from being located in an area with intense transcurrent shear and from the occurrence of pebbles rich in magnetite. Because of paucity of surface geological information, a ground-based geophysical survey added valuable information for the definition of a drilling program in the area. The survey consisted of two parts and followed up the aforementioned previous integrated interpretation of the Valença sheet. The first part consisted of one gravity and magnetic profile, which indicated a favorable site for additional investigation. The second part consisted of a detailed survey in the selected area with gravity, magnetic, and VLF-EM. The interpretation of the data of the geophysical methods allowed to delineate two zones in the area, both located at magnetic anomalies, gravity highs and relatively conductive parts. The two zones have a high potential for iron ore, because they present significant and correlated anomalies.

Key words: Gravity, iron ore, magnetic, VLF-EM.

INTRODUCTION

This work constitutes the second part of a cooperation program between the Center of Research in Geophysics and Geology of Federal University of Bahia and the company Grastone Mineração e Comércio Ltda. The first part consisted of the integrated analysis of geological and airborne magnetic and gamma ray spectrometry data described in Sampaio et al. (2017). It presents the results of the analysis of detailed ground geophysical data, integrated with geological information, in an area selected among eighteen anomalies defined by the interpretation of the airborne data. Sources of these anomalies can serve as magnetic dipoles with a depth of less than 300m, some of them are close or related to magnetic lineaments, and most pertain to regions of low radiometric content.

The study area is in the Brazilian state of Bahia and lies in the collisional transition zone between the Jequié Block (JB) and the Itabuna-Salvador-Curaçá Block (ISCB). These two Archean blocks, together with the Serrinha and Gavião blocks, have collided during the Paleoproterozoic orogenic events that led to the formation of the São Francisco Craton (SFC) in the State of Bahia, Brazil (Barbosa & Sabaté 2004). Collisional transition zones, such as this one, are important for metallic mineralization of possible economic interest, because they constitute favorable sites for the intake of mineralized solutions that may lead to formation of ore deposits, including

iron deposits and banded iron formation (BIF) (Smithies & Bagas 1997, Yu et al. 2005, Hagemann et al. 2007, Beukes et al. 2008).

Though the new interpreted contact between the JB and the ISCB does not cross the area of the selected anomaly, the favorable geologic setting encouraged the conduction of a geological survey because of the occurrence of pebbles rich in both magnetite and oxidized iron-rich minerals and of an intense transcurrent shear zone in and around it. Furthermore, it is possible that there may be remnants of ISCB rocks not detected in the airborne survey.

The extensive cover in the area including Tertiary sedimentary rocks, alluvium, and dense vegetation, results in few outcrops making difficult to map the source of the iron-rich pebbles using traditional geology surveys. So it became necessary to add geophysical surveys to help direct a drilling program. Though granite and ultrapotash rocks may bear iron ores, we didn't find any enrichment of iron in those types of rocks in the area. Therefore, our targets are BIFs (primary) and iron rich mafic-ultramafic rocks (secondary).

We use the term BIF in a loose sense, because there is no occurrence of sedimentary strata in the area. In this paper, BIF means alternating layers with high and low grade of iron oxide in paraderived granulite.

Taking into account the geologic information, we selected three of the anomalies defined by the aforementioned airborne geophysical survey to traverse them with detailed ground gravity and magnetic profiles. The result along one of the profiles justified a ground geophysical survey of the area around it. The survey consisted of gravity, magnetic, and VLF-EM (Very Low Frequency) data collected along W-E lines. We performed the data interpretation of the three geophysical methods in a combined form, to determine targets of economic interest for exploration of iron ore. So, it was possible to delineate two zones of high potential iron ore based on coincident anomalies in the three data sets.

Geologic background

Figure 1 represents the present geological map of the Valença sheet. The geology, adapted from a map at a scale 1:250,000 and based on ground mapping, petrographical analysis of collected samples and geochemical assay in some of them, was improved by integration with the airborne geophysical data interpretation (Sampaio et al. 2017). However, rock outcroppings are scarce and mostly located along drainages and quarries in the area. This restrains the definition of the boundaries between rock units, yielding uncertainty in the geology map.

The geology of the studied area consists mostly of Precambrian rocks that, in the east, are overlain by the Mesozoic Camamu Basin (CB), sedimentary rocks of the Tertiary Barreiras (BF) formation, and Quaternary sediments (Figure 1). The Tertiary and Quaternary sediments also cover the Precambrian rocks in several places to the west. The Precambrian rocks have been metamorphosed to amphibolite and granulite facies and are mapped as two Archean tectonic units: JB on the west and ISCB to the east. They, and the Gavião and Serrinha blocks outside the Valença sheet, collided during the Paleoproterozoic resulting in the ISCB orogeny. The orogeny formed a N-S trending mountain chain that is at least 1000km-long between the cities of Itabuna in the south and Curaçá to the north (Barbosa & Sabaté 2002, 2004). Erosion has exposed the high-grade metamorphic rocks at the core of the orogen.

The JB Block consists of highly deformed and metamorphosed, and sometimes migmatized granulite facies, Mesoarchean rocks. The rocks include both mafic and quartz

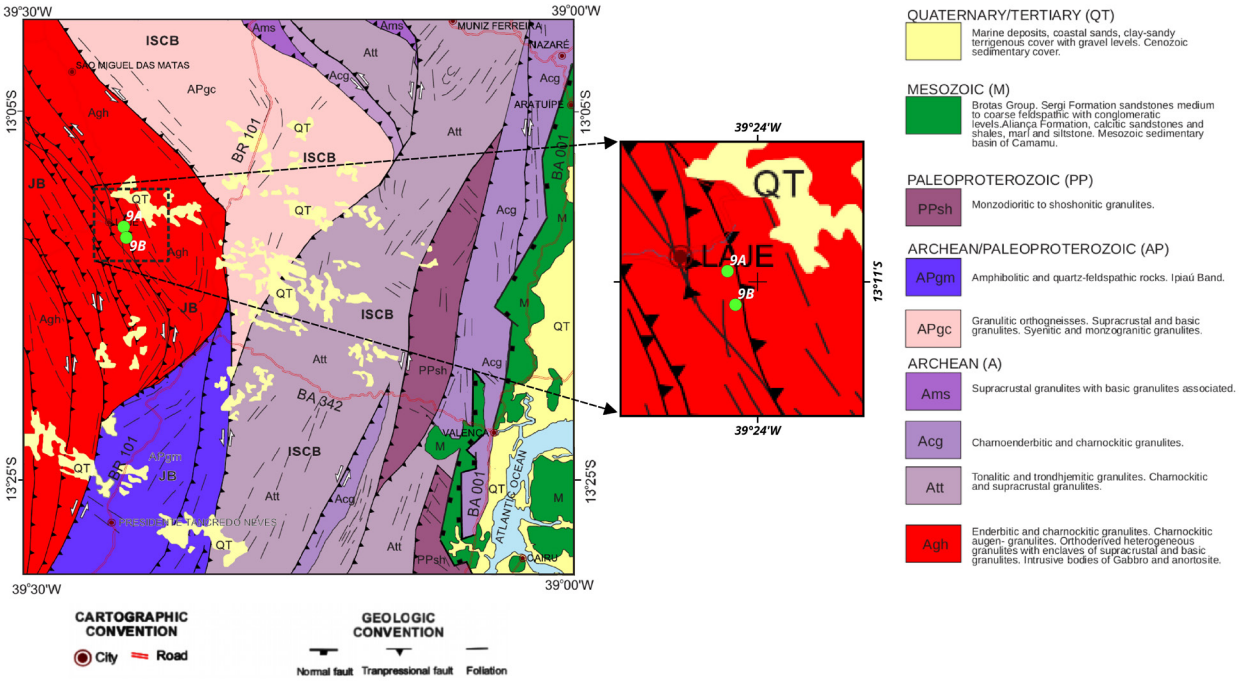

Figure 1. Geological map and legend of the Valença sheet adapted from a map at a scale 1:250,000. Points 9A and 9B are the extreme points of the profile selected for ground-truth investigation. The quadrangle indicates the location of the area of the detailed geophysical survey.

feldspathic rocks, kinzigites, quartzites, and garnet and orthophyroxene-bearing quartzites. Heterogeneous ortho-derived granulites, with enclaves of supracrustal and mafic granulites, and leucocharnockites with garnets and cordierites are also part of this set. The latter lithotypes are products of partial melting of kinzigites formed at the peak of the granulitization. Enderbitic-charnockitic granulites also occur in the JB, mainly outcropping around the city of Laje and extending beyond the southern border of the map.

There are intrusive bodies of gabbro-anorthosite rocks mineralized in Fe-Ti-V in the region where the granulites occur (Cruz 1989), which may be the iron source for the BIFs. Post-tectonic non-deformed and of circular shape charnockites also appear as a dispersed distribution in the area. These intrusive bodies were emplaced during the Paleoproterozoic.

Amphibolite and quartz feldspathic rocks, although part of the JB, are found in the so-called Ipiaú Band, positioned between blocks of granulites: the west side with charnockitic granulites of the JB and the east side with tonalitic granulites of the ISCB. In Figure 1, the Ipiaú Band corresponds to the APgm unit, which is in contact with the Apgc and Att units of the ISCB. They consist of ortho- and paragneisses where intercalations of amphibolites and quartz-feldspathic materials predominate, although quartzites, kinzigites, and BIFs (our primary target) also occur sporadically. These rocks are similar to the orthoderived heterogeneous granulites, with the difference that in the Ipiaú Band they are metamorphosed into the amphibolite facies (Barbosa 1990). Granites are rare in the JB but do occur in the Ipiaú Band.

The ISCB trends N10° E and is composed of granulite facies rocks. In the southern part,

paleoproterozoic monzonite and monzodiorite granulites are found, although most rocks are tonalite-trondhjemite granulites of the Neoarchean and Paleoproterozoic. These rocks are very similar despite their disparate ages, both from the macroscopic point of view and in their mineralogical and petrochemical properties. Tracks containing mafic granulites and paraderived granulites are also found in this block. Both of them form tectonic mega-enclaves in the older tonalite-trondhjemite granulites (Sampaio et al. 2017).

Although they are not our primary target, it is worth mentioning two bodies of mafic-ultramafic rocks: Palestina and Mirabela, because they confirm the metallic potential of the region. Both occur beyond the southern border of the Valença sheet, presumably on the boundary between the JB (Ipiaú Band) and the southern part of the ISCB, which are roughly aligned in the NS direction and mineralized in sulfides of nickel and platinum. Mirabela became recently an important mine of nickel and, secondarily of platinum group metals (PGM).

Figure 1 also shows the approximate position of the points 9A and 9B – northwest and southeast extremes of the ground profile – and the area of the ground survey about 5km southeast of the city of Laje. The ground prospect is within the Agh unit of the JB. Before the study of Sampaio et al. (2017), it was in the vicinity of its limit with the Att unit of the ISCB. After this study, the boundary between the Agh unit of the JB and the APgc unit of the ISCB was moved northeast. However, this does not preclude the possible occurrence of remnants of ISCB unit in the prospecting site. The occurrence of APgc and Ams units of ISCB rocks around the Brejão dome beyond the western border of the Valença sheet and right in the core of the JB – see Figure 13B of Sampaio et al. (2017) – justifies this assumption.

Ground geophysical survey

Gravity and magnetic methods have been used with stations spaced 20m along the profile between the points 9A and 9B having a length of 6600m and a NNW-SSE direction. Based on the interpretation of the gravity and magnetic data of this profile, we decided to conduct a detailed 2D ground survey in an area of about 1.9km^2 with W-E and N-S sides, which is almost longitudinally sectioned by the profile and divided into two subareas: the northern subarea A1 with 0.8km^2 and the southern subarea A2 with 1.1km^2 – see Figure 4. The survey consisted of measurements using gravity, magnetic, and VLF-EM methods with a 20m W-E × 100m N-S grid. We will present the interpretation of the profile and of the 2D survey sequentially. In both cases, we have determined station locations using GPS with precision better than ±10cm in the SIRGAS 2000 UTM coordinates, and ±2cm in their respective ellipsoidal altitudes.

A single GSM-19G Overhouser magnetometer has been used during the survey with a mean square reading estimate precision better than ±1nT. Repeated readings at a reference station along each line accounted for diurnal variation. We also took readings twice each day at a local base station to follow the day to day variation of the ambient field, in addition to verifying that no magnetic storms occurred while conducting the surveys.

Because we had only one magnetometer, we had to set up a procedure to correct the time drift and to link the magnetic readings of the different lines of the 2D survey. Initially, we surveyed the N-S tie-line and occupied one of its stations three times at a time interval of less than 1 hour. Based on a linear regression of the repeated readings, we have determined the final value of every station of the N-S line. We repeated the procedure for each W-E line, choosing as reference station to repeat readings

the one at the intersection with the N-S auxiliary line. We subtracted the value of the ambient field from the resulting values so obtained and applied a low pass filter to delete the high frequency content due to shallow sources.

We collected the gravity data using a CG-5 gravimeter and tied them to absolute values using the Brazilian Network of Gravity Stations (RGFB). Before the survey, a preliminary test at a base station established the automatic static drift compensation. Readings taken twice daily at a local absolute gravity station checked the dynamic drift of the instrument. Adoption of this standard procedure improved the determination of the gravity data at each station. We applied the procedure prescribed by Hinze et al. (2005) to the absolute values, to compute the simple Bouguer gravity values and subsequently applied a terrain correction for the local topography. For the simple Bouguer values, we assume an accuracy of about ±50μGal, because the mean square reading precision is better than ±30μGal and the precision of the elevation measurement is about ±2cm. We estimate a precision at least of ±0.1mGal after the terrain correction.

Analysis of the magnetic and gravity data along section 9A-9B

The station separation along the section was 20m, totalizing 331 readings for both magnetic and gravity data. We assume that the magnetization of the BIF is higher than that of the country rock and the density contrast between the iron enriched bodies and the granites or anorthosites is higher than 500kg/m^3 resulting in well defined magnetic anomalies and gravity highs over those bodies.

Magnetic data

The International Geomagnetic Reference Field (IGRF) of the area at the time of the survey was: magnitude of the ambient field equal to 24,545nT; declination of 23.28° W; and inclination of -30.58°. The profile is masked by strong negative values at stations 2120m and 2300m due to the presence of very shallow magnetic sources – magnetic pebbles – at those two stations. To avoid the interference of those values, we represent the variation of the residual magnetic data for the entire profile after removing those two values (lower than -700nT) in Figure 2a. Figures 2b, c and d represent the variation of the residual magnetic data, respectively, of the northern, central, and southern parts of the profile without removing those data as is evident in Figure 2c. The residual data equals the observed value minus the local magnitude of the ambient field.

We have identified five distinct anomalous magnetic zones along the 9A-9B profile from north to south. Each zone relates to a distinct content of iron oxide resulting in unspecified and mostly subtle lithological differences.

Zone 1 is located between the positive peaks at stations 80m and 840m (Figure 2b). It contains a sequence of peaks and troughs all of them with values lower than -100nT. Its variation seems to result of relatively narrow sources, because the wavelength (Blakely 1996) varies between 120m and 200m.

Zone 2 is located between stations 900m and 1340m (Figure 2b). It is narrower than Zone 1, but also presents peaks and troughs with negative values and short wavelength values that indicate narrow sources. Two magnetic sources centered at stations 1020m and 1180m are the main anomalies of this zone.

Zone 3 is located between stations 1440m and 2820m (Figures 2b and c). Strongly magnetized bodies must occur at a very shallow depth around stations 2120m and 2300m. These are important anomalies. The negative anomalies both characterized by one peak flanked by two

troughs and centered, respectively, at stations 1600m and 2800m are also important.

Zone 4 is located between stations 2820m and 5300m (Figures 2c and d). It presents a long wavelength magnetic high superimposed by a low amplitude magnetic low between stations 4240m and 4600m. This zone is possibly associated with a non magnetized charnockite.

Zone 5 is located south of station 5300m (Figure 2d). There is a sharp increase in magnetic values between this and Zone 4. Zone 5 certainly extends beyond the SSE limit of the profile. Figure 2d displays 3 prominent narrow magnetic lows located at stations 5700m, 6040m, and 6420m.

The ground data discriminate and locate the sources more precisely than the airborne data for the first two zones. Furthermore, the airborne data were unable to recognize the third anomalous zone, as well as the step between the fourth and the fifth zone, which suggests a sharp contact between two very distinct lithologies.

Gravity data integrated with the magnetic data

Figure 3a displays the variation of the Bouguer value of the entire profile. We have identified

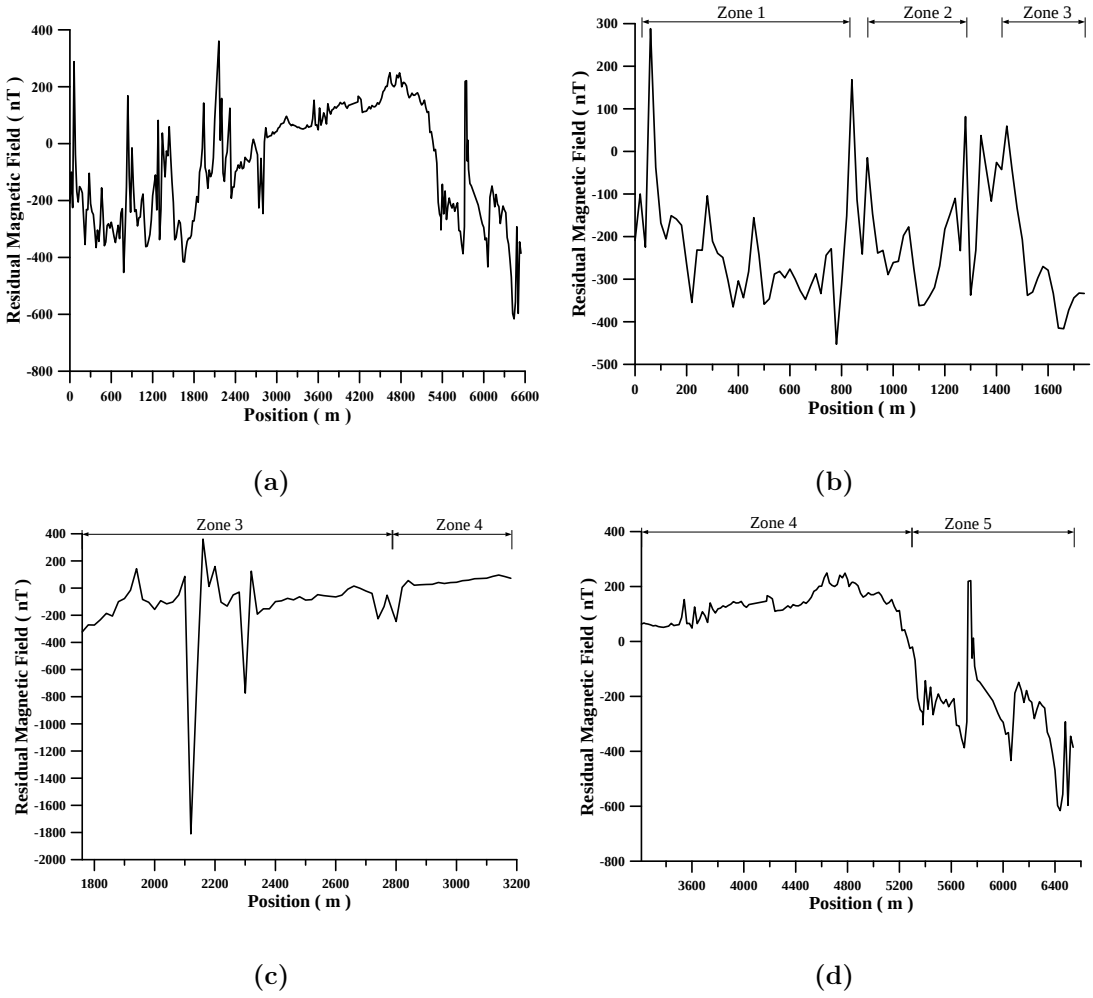

Figure 2. Variation of the residual magnetic values along the NNW-SSE profile – observed value subtracted of the ambient field: (a) for the entire profile after exclusion of anomalous values lower than -700nt; (b) for its northern part; (c) for its central part; (d) for its southern part.

three gravity zones in Figures 3b and c that display, respectively, the variation of the Bouguer value of the northern and the southern parts of the profile.

Zone 1 extends between the NNW limit and station 960m. It presents three relatively large gravity highs and the southernmost of them has a residual value of almost 6mGal. So, it contains an anomaly, which characterizes a lithology denser than the neighboring rocks. Since the magnetic field also oscillates intensively along it, this association suggests the occurrence of iron rich bodies under the weathered cover, possibly BIFs, along an extension of 800m.

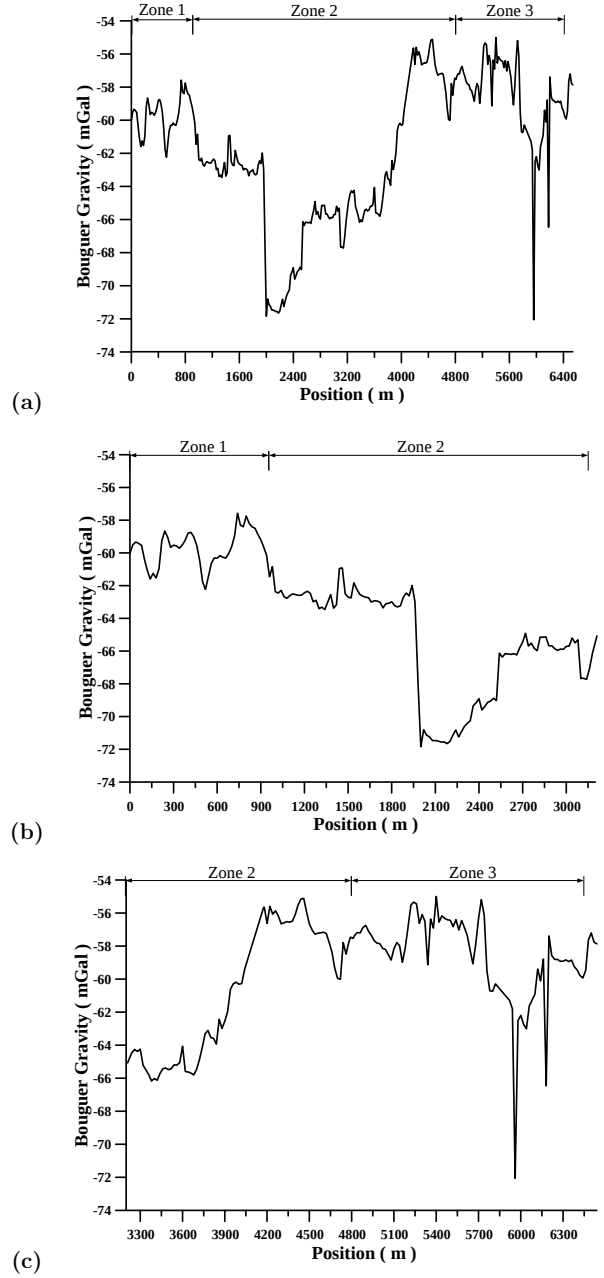

Figure 3. **Variation of the Bouguer gravity values along the NNW-SSE profile: (a) for the entire profile; (b) for its northern part; (c) for its southern part.**

Zone 2 occurs between stations 960m and 4080m. It contains a gravity anomaly between stations 2520m and 3120m with a residual value of 2.5mGal correlated to a magnetic anomaly of -220nT between stations 2700m and 2820m.

Zone 3 extends from station 4080m up to the SSE limit of the profile and displays the highest residual values in two stretches, which are separated by a 200m wide trough centered, approximately, at station 6040m. The SSE stretch contains two residual gravity highs. Though their values are relatively small, they coincide with part of the magnetic oscillation of large negative amplitude (between -200nT and -500nT). So, this stretch may be associated with alternating bands enriched with iron oxide. The NNW portion of Zone 3 contains the largest Bouguer anomalies with residual values of up to 4mGal. The anomaly close to the northern limit of the zone coincides with the relatively calm magnetic zone. This association suggests the presence of rocks of more mafic composition, but relatively depleted in magnetite. The other segment with high Bouguer values, in this portion of Zone 3, occurs between stations 5400m and 5700m. It coincides with an intense magnetic oscillation of low peak-to-peak amplitude and negative values. Again, this association suggests the possible presence of BIF bands here.

Geophysical analysis of the detailed area

Topographic survey

The topographic plan of the area of the ground geophysical survey consists of a 20m W-E × 100m N-S grid with a total of 1,051 stations along 21 W-E lines. A N-S tie-line served as link to level the magnetic data and help to control its time drift. Figure 4 represents the topography. It displays both the grid and the elevation of the area, obtained by the GPS survey. We have numbered 01 and 21, respectively, the southernmost and the northernmost lines. The survey area was limited because of an environmentally protected region on its southwest side. Line 11 serves as a limit between the northern part – subarea A1 – and the southern part – subarea A2.

Magnetic method

Figure 5 is the low pass filtered magnetic map for a filter length of 80m or half the Nyquist frequency ($0.0125m^{-1}$) along each W-E line. The contribution of the very shallow or surficial sources is filtered out or smoothed on the map. However, the resolution is still adequate to delineate relatively shallow sources because of the relatively high cutoff frequency. This is evident for the anomaly between stations 1160m and 1280m of Line 5 of A2, where two neighbor

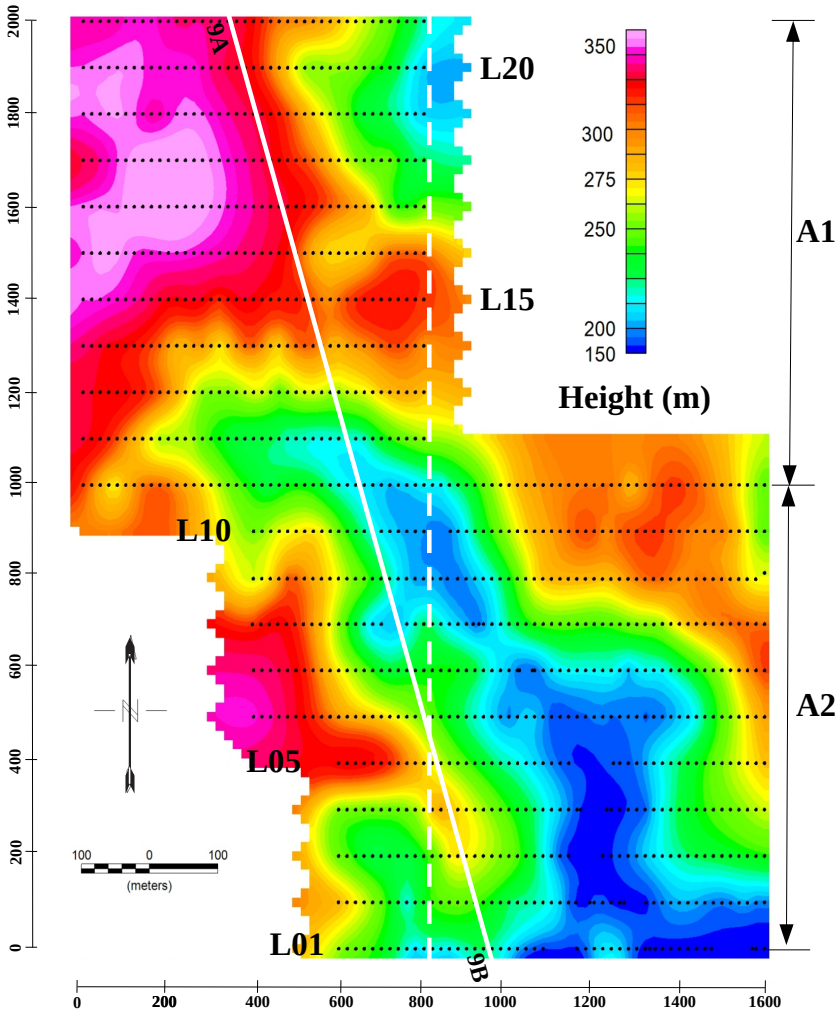

Figure 4. Topographic map of subareas A1 and A2 showing the distribution of W-E lines and stations, the NNW-SSE profile (white solid line), and the N-S tie-line for the magnetic data (dashed white line).

bodies are individualized (see red circle in Figure 8a). Data with a cutoff frequency equal to one-fourth of the Nyquist frequency didn't individualize them.

If we surveyed a square instead of a rectangular grid, employed three instead of one tie-line, and applied a 2D filter instead of filtering along each line, we would achieve a better accuracy (close to ±1nT). However, for the purpose of the survey, the levelling of the magnetic data is satisfactory.

Interpretation

It is well known that the shape of the magnetic anomalies depends on the declination and inclination of the ambient field. The magnetic map (Figure 5) clearly defines two regions, which must correspond to two distinct geological environments. The first one occupies almost all of A1 and the NE part of A2 and the second one occupies a small southwestern part of A1 and more than 80% of A2.

The boundary between these two regions follows the sequence of magnetic troughs of the magnetic map and consists of two parts. The first part has a N60° W trend from the eastern limit to the central part of the map. The second part is shorter and trends ENE-WSW from the central part towards the western limit of the map. Figure 8a constitutes a map integrating the main structural features observed in the magnetic map and displays the trace of this boundary.

The first region is highly inhomogeneous with E-W oriented small magnetic dipoles and large isolated magnetic highs and lows, up to +270nT and down to -120nT respectively. The spread of these anomalies is superimposed on E-W lineaments. The dipoles are mostly on the eastern side of A1, distributed between lines 15 and 20. The dipole anomalies along Line 17 correspond to an outcropping pegmatite and the isolated anomalies along Line 12 constitute, partially, a transition zone into the second region. Another sequence of E-W oriented small dipole anomalies occurs on lines 9, 10, and 11, on the NE side of the boundary of the two regions. Possibly, the source of the dipole anomalies are magnetite enriched pools of the country rock, whereas the isolated anomalies reflect larger magnetic bodies. The relatively high magnitude of the anomalies does not favor deep sources in either case.

The second region contains an important NW-SE lineament parallel to the boundary between the two regions. This lineament extends from station 1320m of Line 1 to station 400m of Line 8 and divides the second region into two parts. In the southwest, the magnetic values are mostly higher than +60nT and this subregion seems to pertain to a highly homogeneous geological environment. It also contains the most important magnetic anomaly of A2 between lines 1 and 4, with an amplitude higher than 180nT and at least 300m wide. The northeastern part is less homogeneous and contains, besides the aforementioned positive anomaly in Line 5, some low values – between -18nT and +35nT – as for instance, around stations 1480m of Line 6, 1380m of Line 4, and 1440m of Line 3. Its behavior suggests the occurrence of several iron enriched pools.

Figure 8a shows the position of the dipoles and lineaments described for the two regions. We point out that both magnetic troughs and peaks are important for iron prospection because of remanence in BIF's.

Gravity method

The Bouguer and the residual gravity maps are displayed, respectively, in Figures 6 and 7.

Interpretation

The Bouguer map shows two distinct regions. The first one covers most of A1 but continues into the northeastern corner of A2 and shows low Bouguer values predominantly. It must correspond, mostly, to thicker overburden, to the coverture of the BF, and to the granulite with the presence of silicate-rich rocks, eventually pegmatites, that are locally enriched in iron. Most of the second region presents high values and occupies a small SW portion of A1 and almost all of A2. We interpret it as corresponding to the domain of rocks with mafic composition intercalated with BIF.

The -60mGal value of the Bouguer map marks the boundary between the two regions, which extends along two lineaments: (i) in the N45° E direction between lines 11 and 13 at the west of A1; (ii) in the N60° W direction, approximately, from station 320m of Line 13 of A1 to the east of Line 6 of A2. Three other lineaments also occur. The first one cuts the limit of the two regions between station 340m of Line 11 and the extreme east of Line 17 of A1 along the N45° E direction. The other two belong to the second region. The second one is along the N-S direction between lines 6 and 10 at the west limit of A2 and the third one coincides with the distribution of peaks to the south of A2 and is along the N45° W direction. The boundary and the lineaments are displayed in Figure 8b.

Location of gravity anomalies is important because the troughs imply the presence of unconsolidated or more sialic material and the peaks imply the presence of dense lithotypes. Also, metallic mineral deposits may be dense and produce gravity anomaly highs.

We have identified 4 troughs (g_B < −62mGal) and 4 peaks (g_B > −60mGal) in the first region and 2 troughs (g_B < −61mGal) and 4 peaks in the second region. They are located in Figure 8b. The most significant peaks of the Bouguer map are those located between stations 660m of Line 3 and 820m of Line 1 of A2 and between stations 1200m of Line 4 and 1300m of Line 2 of A2.

We calculated the residual gravity anomaly by removing a linear trend in the data. The trend removal aimed, primarily, to smooth out from the Bouguer map the contribution of the difference of density between the JB and the laterally positioned ISCB and Ipiaú Band. Though the Regional also contains contribution of deep crustal sources, the area is too small to register lateral variations of gravity (due to them) larger than due to the aforementioned blocks. So, it is important to describe and analyze both Bouguer and Residual data. In rough terms, the Bouguer enhances the geological framework and the Residual the pools of more dense rocks, such as mafic or BIF.

The residual gravity map, represented in Figure 7, shows four regions: two in subarea A1 separated by an almost N-S boundary; one spreading from the south of A1 up to the middle of A2; and one in the southern part of subarea A2. Other than that, the residual map confirms several of the peaks of the Bouguer map. The residual map also stresses the importance of the southern part of A2 where several anomaly highs are isolated from the broader Bouguer anomaly (Figure 6). Besides, the residual map shows a prominent anomaly in the northeast part of A1, where there is a wide domain of relatively positive anomalies having values larger than 1,500μGal.

These aspects described for the residual are also displayed in Figure 8b. The display of the magnetic and gravity lineaments and anomalies side-by-side serves to confirm the good correlation between these two geophysical methods and their ability to distinguish the geological environments present in the area.

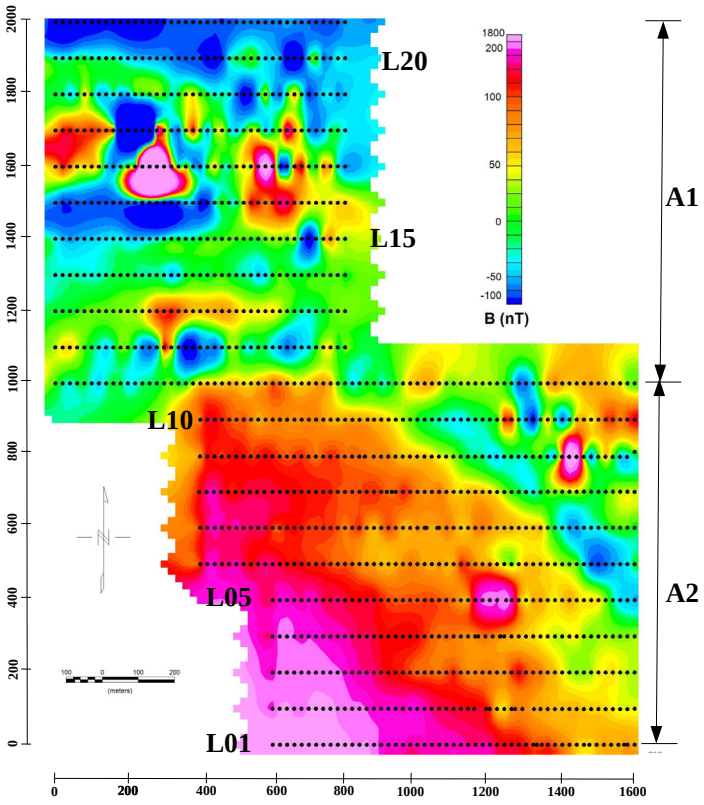

Figure 5. Magnetic map of subareas A1 and A2: data filtered for a frequency equal to one half of the Nyquist frequency.

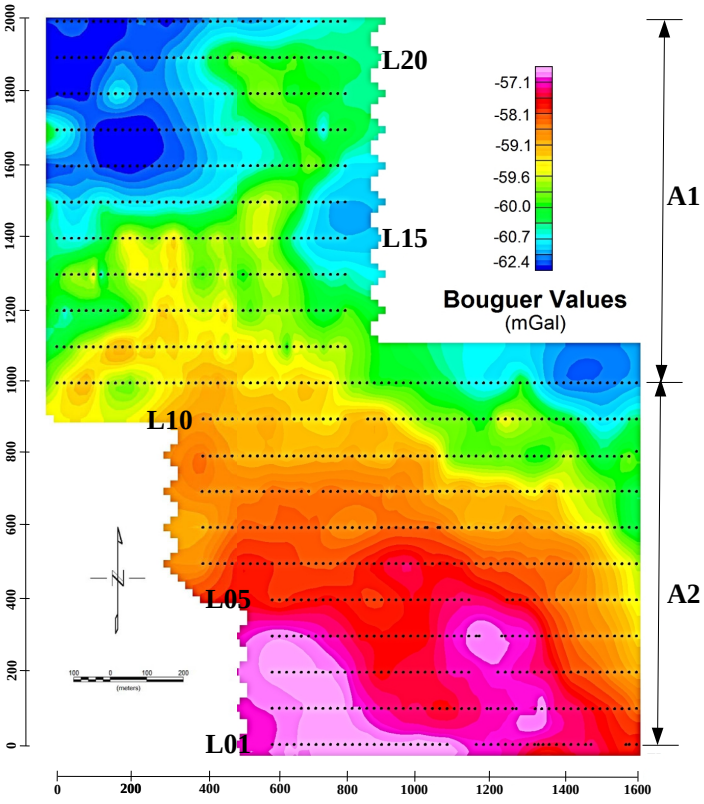

Figure 6. Bouguer gravity map of subareas A1 and A2.

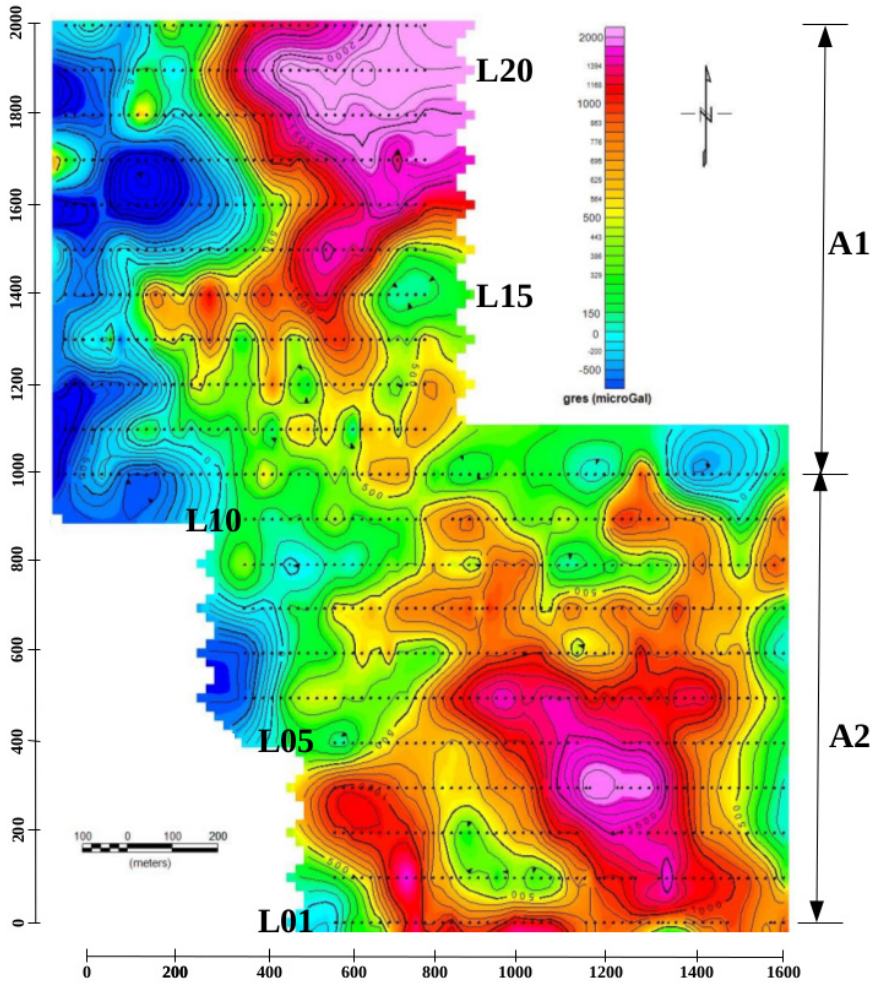

Figure 7. Residual gravity map of subareas A1 and A2.

Quantitative modeling

To exemplify the quantitative analysis that may help defining a drilling program we performed: (a) the joint 2D magnetic and gravity modeling of Line 3 and the 3D gravity modeling of subarea A2. The area has not been the subject of either detailed geological mapping or prospective drill-hole programs. Therefore, there are no objective constraints and we had to rely on the scarce knowledge of the lithology and assume published values of the physical properties.

Figure 9 displays the 2D modeling of Line 3, which employed an ordinary Geosoft™ modeling package. We are aware of the limitation of this modeling because the bodies are not truly 2D and their strikes are not N-S.

The quantitative interpretation adopted used Euler Deconvolution initially. It involves the determination of the position of the causative body based on an analysis of the fields and their gradients and constraints on the geometry of the causative bodies. It didn't take into account remanence or self-demagnetization for the magnetic model.

The quality of the depth estimation depends mostly on the choice of the proper structural index which is a function of the geometry of those bodies and adequate sampling of the data (Williams et al. 2005). In this study, a structural index of 0.5 was adopted since it gives the most

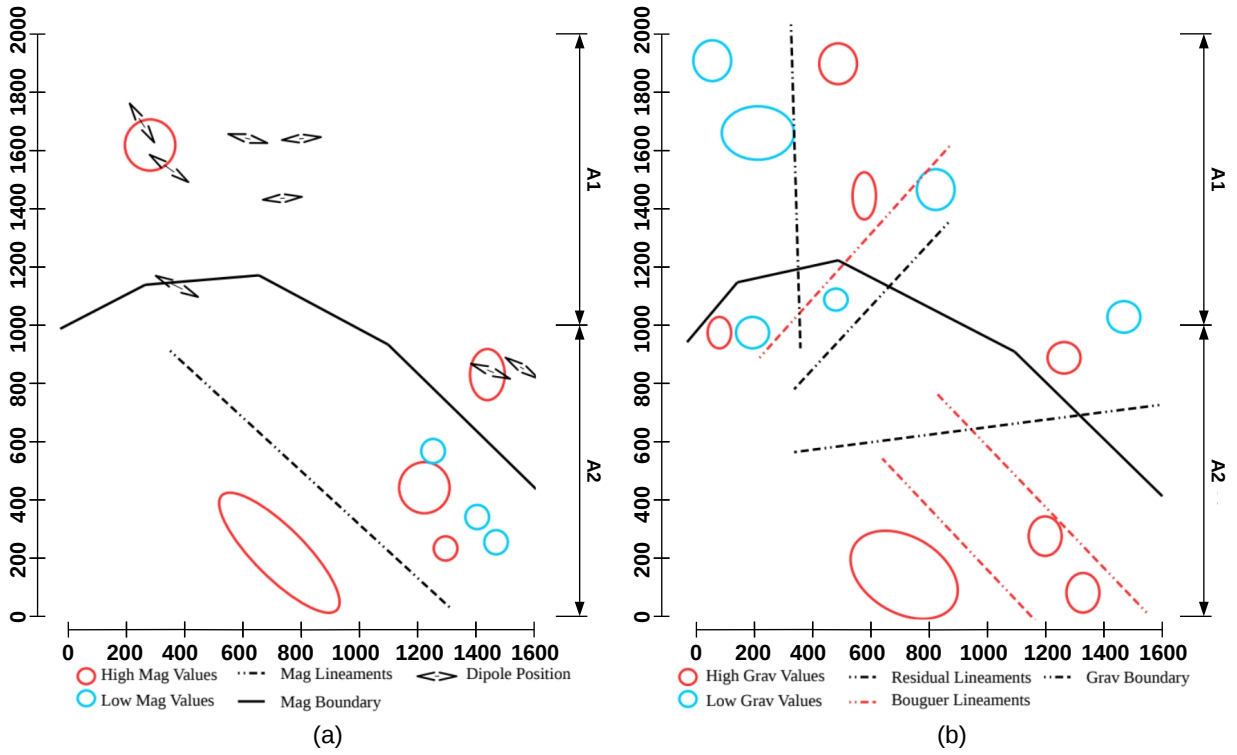

Figure 8. Display of the structural features of the area based on: (a) the magnetic and (b) the gravity data.

accurate depth estimates for the magnetic data where the typical source structures are of finite offsets. Well clustered Euler solutions were obtained at a shallow depth of approximately 100-300m. The parameters obtained from the Euler deconvolution were used as the startup parameters for 2D forward modeling. The modeling allowed to define the values of the density and of the susceptibility of a basement rock overlain by 9 east dipping bodies.

For depths larger than 260m, the values indicate a non magnetic lithology with a density close to the average value of the continental Crust, implying a felsic composition for the basement. Density decreases for distances larger than 840m (bodies B8 and B9) and susceptibility decreases for distances larger than 620m (bodies B6, B7, B8, and B9). This suggests a progressive enrichment of felsic composition and impoverishment of magnetic minerals towards the east of the profile. The low density of B3 (d < 2.5g/cm^3) and high susceptibility (χ = 0.006CGS) may indicate a fractured and weathered zone of mafic lithology with apport of metallic minerals, inasmuch that it is bounded by the dense and magnetic bodies B2 and B4.

Figure 10 shows the variation of a 3D linear inverse density model of subarea A2 and the respective map of the residual gravity. The modeling computed the density values of 208 homogeneous prisms of the same size and fixed vertices. Their horizontal sides are 40m E-W × 100m N-S, tops are 5m deep and basis are 105m deep. The bases of the prisms have been set at 105m after some trials, mainly because the resolution of the inversion is poor for larger depths.

A comparison between Figures 7 and 10 shows that the density distribution of the 3D prismatic bodies reproduces with great fidelity the variation of the residual gravity of subarea A2. It also complies, approximately, with the density

model shown in Figure 9. Therefore, despite the limitations of the 2D and 3D modeling, they serve to support and confirm the qualitative analysis.

VLF-EM method

VLF-EM is a far field non-controlled artificial source electromagnetic method, which presents a small depth of exploration (McNeill & Labson 1991). Its main application aims to define the position of the top either of dipping contacts between two rocks with distinct values of electrical conductivity or of fault zones.

We used a T-VLF in the survey to measure the tilt and the ellipticity of both the vertical and the horizontal polarization ellipse of the magnetic field at two values of frequency: 16kHz and 24kHz. However, the data for the horizontal ellipse and the frequency of 24kHz were noisy and didn't add significant information. Therefore, we used only the tilt of the vertical ellipse for 16kHz after application of a Fraser filter, which changes a cross-over into a peak (Karous & Hjelt 1983). The quality of every employed data is about 90% as registered by the equipment. Taking into account the characteristics and limitations of the VLF-EM data, the achieved results are satisfactory.

Interpretation

Based on the intensity and the signature of the anomalies, it is possible to correlate them with the other two geophysical methods. Specifically, plots of the VLF-EM data may show conductive lineaments, linking cross-over positions, that may be associated with sheared contacts, fault zones, or elongated veins.

Figure 11 displays the contour map of the aforementioned Fraser filtered data (Fraser 1969, Karous & Hjelt 1983). Because VLF is a non-controlled source far field EM method, its measurements are not, statistically, as consistent as the gravity and the magnetic data. However, the Fraser filter pointed out many lineaments (along the peaks) that may indicate fracture zones or sheared contacts through which mineral solutions may migrate. Our interest is in those "conductors" related to the gravity and the magnetic anomalies. We believe that the positive association of the three methods is an important indication of favorable areas for further exploration work for iron bodies. So, we have attributed a relative importance to the positive peak values of the Fraser filtered tilt data in the choice of drilling targets together with the gravity and magnetic anomalies. The positive peaks relate to conductive zones, which may be associated with metallic mineralization.

DISCUSSION

To help in the decision of the drilling targets, we have attributed percentual values to each geophysical method proportional to their importance. The choice of the values is highly subjective and other interpreters may attribute different percentages. They may be thought of as *a priori* Bayesian percentages, which would be changed during a search procedure. In our understanding, locations with magnetic anomalies are the most important places and locations without magnetic anomalies are the least important places. So, we graded those places, respectively, 75% and 10%. Gravity anomalies are the second in importance and VLF Fraser anomalies are the least important of the three geophysical methods. So, we have graded them accordingly.

Table I contains those values as well as their correlation for the three methods. Figure 12 displays the distribution of these correlation values in the area in quadrangles of 100m × 100m. The quadrangles with higher percentual values - ABC and ABc - correspond to the parts of the map with a higher probability of success.

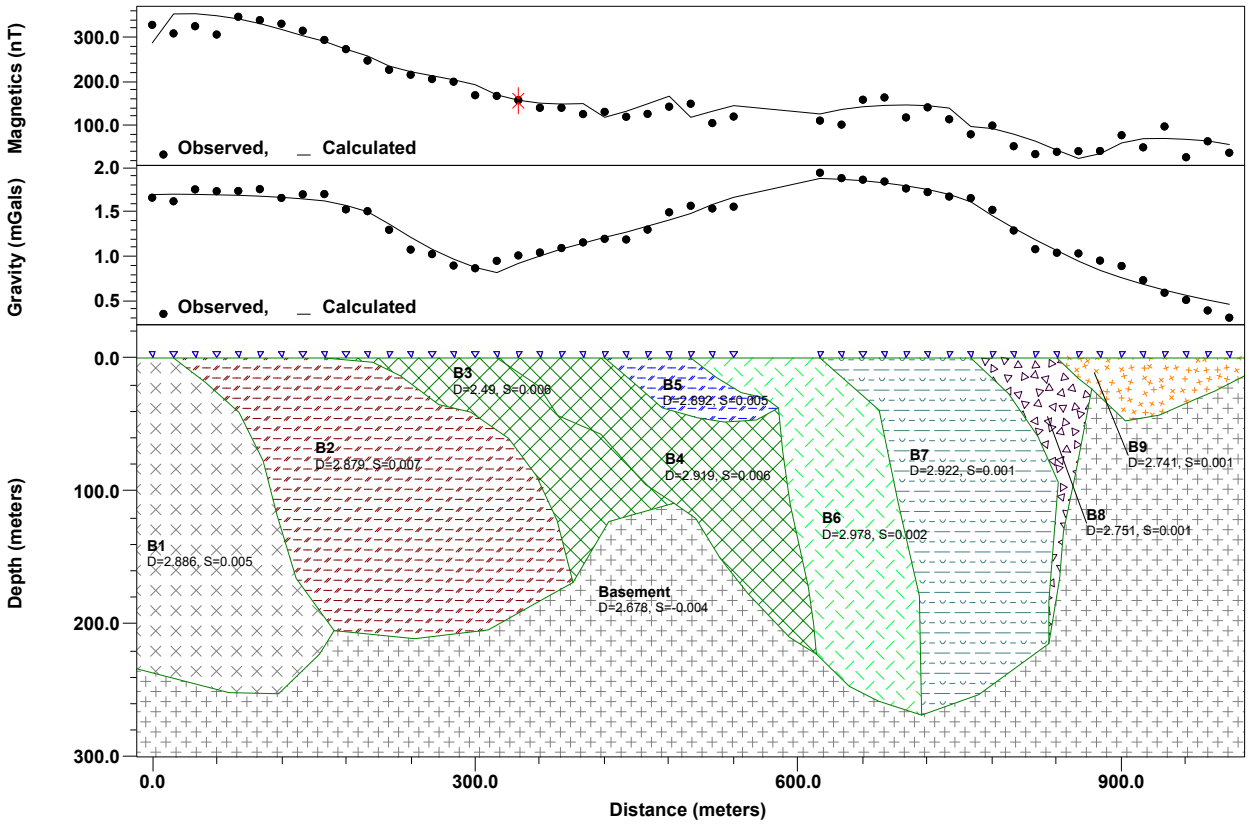

Figure 9. Joint magnetic and gravity modeling of Line 3. Numbers on the polygons represent, respectively, the magnetic susceptibility in CGS and the density contrast in g/cm^3. Distance 0 corresponds to station 600m and distance 1000 corresponds to station 1,600m.

CONCLUSION

The survey helped to better characterize subsurface geology. The magnetic data improved the resolution of neighboring bodies and densified the information both along the profile and in the 2D survey. The gravity method added information about the contrast of mass and defined better the location of the causative bodies.

The combined qualitative analysis of the geophysical data improved the geological knowledge of the prospected area. A preliminary quantitative magnetic and gravity modeling helped in the definition of the targets. We assume that rocks with density contrasts higher than 0.5g/cm^3 relative to the average density of the continental Crust (2.67g/cm^3) may be mafic or ultramafic or contain an appreciable amount of metallic minerals and rock beds with values of χ > 0.03CGS may contain more than 10% of iron oxides.

The 3D modeling of subarea A2 suggests the presence of those high density bodies. Two facts contribute for the smaller values of density determined by the 2D model of Line 3: they represent average values for a mass constituted of several beds alternating between rich and poor metallic content; and the causative bodies neither are truly 2D nor their strikes are orthogonal to Line 3.

The gravity, magnetic, and VLF-EM geophysical detailed mapping of the area yielded the individualization of two environments. One,

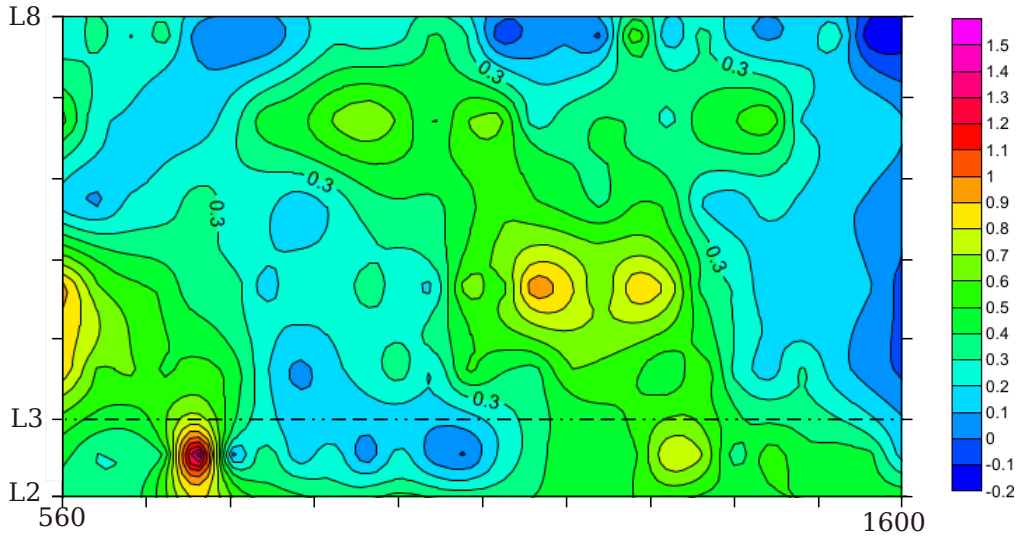

(a)

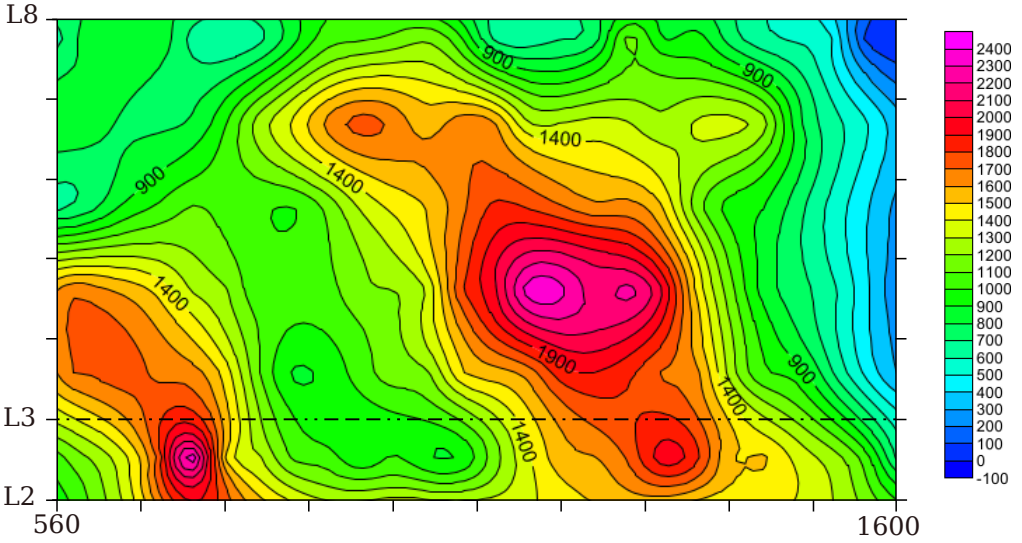

(b)

Figure 10. Gravity modeling of subarea A2. (a) Variation of the density, in g/cm^3, of 208 prismatic bodies with tops 5m deep, bases 105m deep and horizontal sides 40m E-W × 100m S-N. (b) Respective modelled residual gravity in *μ*Gal.

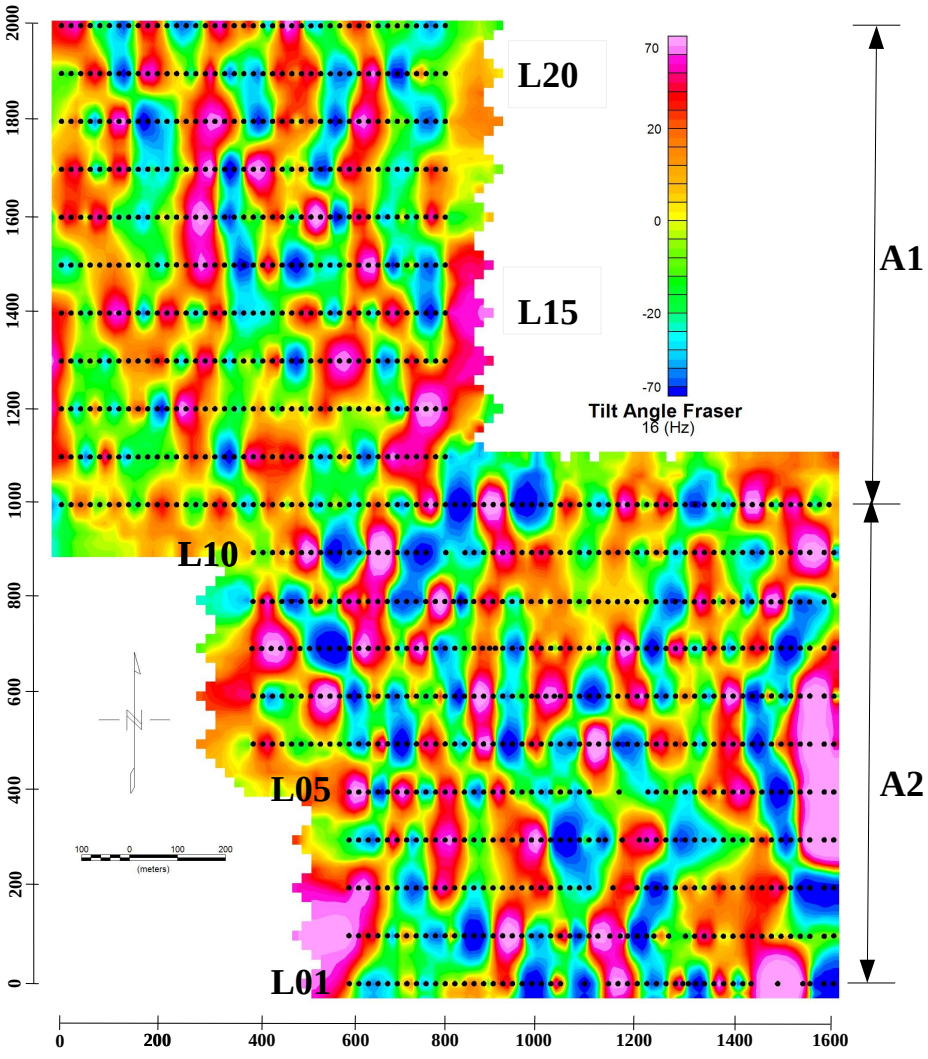

Figure 11. VLF-EM map of A1 and A2: Fraser filter applied to the tilt angle data for 16kHz.

Table I. Correlation of the geophysical anomalies. A: high magnetic peak or trough. a: magnetic background. B: gravimetric peak. b: gravimetric trough or gravimetric background. C: Fraser peak. c: Fraser trough or Fraser background.

	Magnetic (%)	Gravimetric (%)	VLF Fraser (%)
With anomaly	**A** = 75	**B** = 60	**C** = 45
Without anomaly	**a** = 10	**b** = 20	**c** = 30
Correlation	(%)	(%)	(%)
A B C	20.25	a b c	0.6
A B c	13.50	a B C	2.70
A b c	4.50	a B c	1.80
A b C	6.75	a b C	0.90

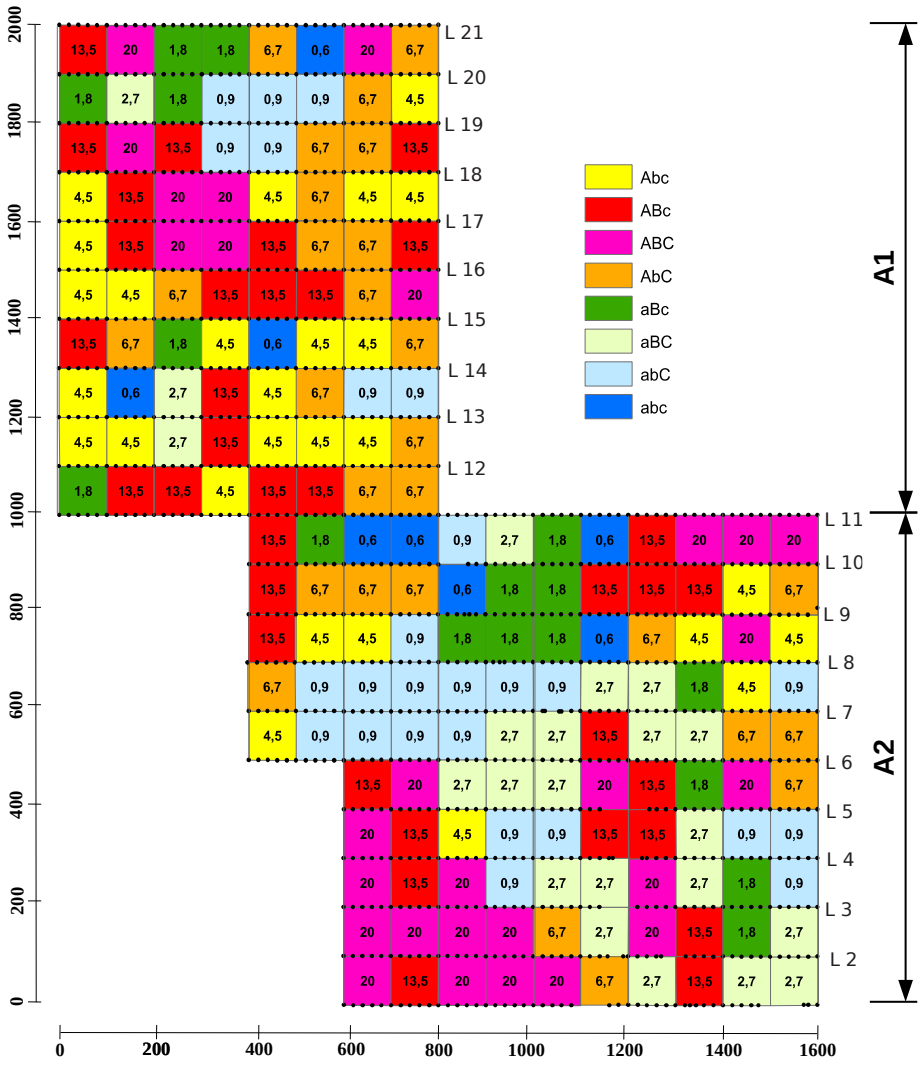

Figure 12. Map of classification of priority areas for drilling programs.

predominantly dense and magnetic, is limited by conductive faults and occupies the central and western portions of subarea A2: the southern part of the map. The other, less dense and under the weathered cover, also contains magnetic and conductive bands and occurs in subarea A1: the northern part of the map.

The information of Table I and Figure 12 helps in the decision of establishing a drilling program aided by the fit between the geophysical and the surface geological data. The joint analysis of the geophysical data allowed to confirm the potential of the area for the exploration of iron ores, mostly in A2, but with some important zones also in A1.

Acknowledgments

Grastone Mineração e Comércio Ltda supported the ground survey. L. Pereira and L. Mocitaiba helped, respectively, in the magnetic and VLF-EM surveys. E. Sampaio acknowledges the PQ-SR fellowship from Conselho Nacional de Desenvolvimento Científico e Tecnológico (CNPq).

REFERENCES

BARBOSA JSF. 1990. The granulites of the Jequié complex and Atlantic mobile belt, southern Bahia, Brazil - an expression of Archean Proterozoic plate convergence. *In*: Granulation and crustal evolution, Clermont Ferrand, FR, Springer-Verlag, Nato Science Series C 311, Vielzeuf D & Vidal PH (Eds).

BARBOSA JSF & SABATE P. 2002. Geological features and the Paleoproterozoic collision of four Archean crustal segments of the São Francisco Cráton, Bahia, Brazil: a synthesis. An Acad Bras Cienc 74: 343-359.

BARBOSA JSF & SABATE P. 2004. Archean and Paleoproterozoic crust´ of the São Francisco Cráton, Bahia, Brazil: geodynamic features. Precambrian Res 133: 1-27.

BEUKES NJ, MUKHOPADHYAY J & GUTZMER J. 2008. Genesis of high-grade iron ores of the Archean iron ore group around Noamundi, India. Econ Geol 103: 365-386.

BLAKELY JB. 1996. Potential theory in gravity & magnetic applications, Chapter 11. Cambridge University Press.

CRUZ M. 1989. Le massif du Rio Piau: une intrusion de nature gabbroique et anortositique dans les terrains granulitiques du noyau Jequié-Bahia-Brésil, 280 f. Doctor Thesis - Université Pierre et Marie Curie, Paris, France.

FRASER DC. 1969. Contouring of VLF-EM data. Geophysics 34: 958-967.

HAGEMANN SH, DALSTRA I, HODKIEWICZ P, FLIS M, THORNE W & MCCUAIG C. 2007. Recent advances in BIF-related iron ore models and exploration strategies. Proceedings of Exploration, 5th Decennial International Conference on Mineral Exploration, edited by B. Milkereit 7: 811-821.

HINZE W ET AL. 2005. New standards for reducing gravity data: The North American gravity database. Geophysics 70: J25-J32.

KAROUS M & HJELT SE. 1983. Linear filtering of VLF dip-angle measurements. Geophys Prospect 31: 782-794.

MCNEILL JD & LABSON VF. 1991. Geological mapping using VLF radio fields. In: Nabighian MN (Ed), Electromagnetic Methods in Applied Geophysics, chapter 7, part B, 2, Application: SEG Investigation in Geophysics 3: 521-640.

SAMPAIO ESS, BARBOSA JSF & CORREA-GOMES LC. 2017. New insight on the paleoproterozoic evolution of the São Francisco Craton: Reinterpretation of the geology, the suture zones and the thicknesses of the crustal blocks using geophysical and geological data. J South Am Earth Sci 76: 290-305.

SMITHIES RH & BAGAS L. 1997. High pressure amphibolite-granulite facies metamorphism in the Paleoproterozoic Rudall Complex, central Western Australia. Precambrian Res 83: 243-265.

WILLIAMS SE, FAIRHEAD JD & FLANAGAN G. 2005. Comparison of grid Euler deconvolution with and without 2D constraints using a realistic 3D magnetic basement model. Geophysics 70: 13-21.

YU X, MO X, ZHAO X, ZHOU S & ZENG P. 2005. Possible causes for large-scale mineralization in the Lanping area, western Yunnan: new evidence from Cenozoic igneous rocks and mantel xenoliths. Mineral Deposit Research, Meeting the Global Challenge, Proceedings of the 8th Biennial SGA Meeting Beijing, China, p. 1275-1277.

How to cite
SAMPAIO EES, BATISTA JC & SANTOS ESM. 2021. Interpretation of geophysical data for iron ore detailed survey in Laje, Bahia, Brazil. An Acad Bras Cienc 93: e20200178. DOI 10.1590/0001-3765202120200178.

Manuscript received on February 12, 2020;
accepted for publication on July 8, 2020

EDSON E.S. SAMPAIO
https://orcid.org/0000-0003-3899-3426

JOELSON C. BATISTA
https://orcid.org/0000-0001-9256-6586

EMERSON S.M. SANTOS
https://orcid.org/0000-0001-9200-0822

Universidade Federal da Bahia, Instituto Rua Barão de Geremoabo, s/n, Campus Universitário de Ondina, Ondina, 40170-290 Salvador, BA, Brazil

Correspondence to: **Edson Emanoel Starteri Sampaio**
E-mail: starteri@ufba.br

Author contributions

Edson Sampaio – (1) Conceptualization of the research. (2) Processing of the VLF-EM data. (3) Three-dimensional modeling of the gravity data. (4) Integrated interpretation of the data. (5) Final writing.
Joelson Batista – (1) Final processing of the gravity and magnetic data. (2) Two-dimensional modeling of the gravity and magnetic data. (3) Integrated interpretation of the data. (4) Partial writing.
Emerson dos Santos – (1) Acquisition of the geophysical data. (2) Preprocessing of the gravity and magnetic data. (3) Integrated interpretation of the data. (4) Partial writing.